

Two-dimensional wave-front reconstruction from lateral shearing interferograms

Peiying Liang¹, Jianping Ding¹, Zhou Jin¹, Cheng-Shan Guo², and Hui-tian Wang¹

¹ Department of physics, Nanjing University, Nanjing 210093, China

² Department of Physics, Shandong Normal University, Ji'nan 250014, China
jpding@nju.edu.cn

Abstract: An algorithm is proposed to reconstruct two-dimensional wave-front from phase differences measured by lateral shearing interferometer. Two one-dimensional phase profiles of object wave-front are computed using Fourier transform from phase differences, and then the two-dimensional wave-front distribution is retrieved by use of least-square fitting. The algorithm allows large shear amount and works fast based on fast Fourier transform. Investigations into reconstruction accuracy and reliability are carried out by numerical experiments, in which effects of different shear amounts and noises on reconstruction accuracy are evaluated. Optical measurement is made in a lateral shearing interferometer based on double-grating.

©2006 Optical Society of America

OCIS codes: (120.3180) Interferometry; (120.5050) Phase measurement; (070.2590) Fourier transform.

Reference and links

1. W. J. Bates, "A wavefront shearing interferometer," *Proc. Phys. Soc.* **59**, 940-952(1947).
2. V. Ronchi, "Forty years of history of a grating interferometers," *Appl. Opt.* **3**, 427-450(1964).
3. M. V. R. K. Murty, "The use of a single plane parallel plate as a lateral shearing interferometer with a visible gas laser source," *Appl. Opt.* **3**, 531-534 (1964).
4. M. P. Rimmer, "Method for evaluating lateral shearing interferograms," *App. Opt.* **13**, 623-629(1974).
5. M. P. Rimmer and J. C. Wyant, "Evaluation of large aberration using a lateral-shear interferometer having variable shear," *App. Opt.* **14**, 142-150(1975).
6. R. R. Gruenzel, "Application of lateral shearing interferometry to stochastic inputs," *J. Opt. Soc. Am.*, **66**, 1341-1347(1976).
7. R. S. Kasana and K. J. Rosenbruch, "Determination of the refractive index of a lens using the Murty shearing interferometer," *Appl. Opt.* **22**, 3526-3531 (1983).
8. T. Yatagai and T. Kanou, "Aspherical surface testing with shearing interferometer using fringe scanning detection method," *Opt. Eng.* **23**, 357-360 (1984).
9. T. Nomura, K. Kamiya, S. Okuda, H. Miyashiro, K. Yoshikawa, and H. Tashiro, "Shape measurements of mirror surfaces with a lateral-shearing interferometer during machine running," *Precis. Eng.*, **22**, 185-189 (1998).
10. L. Erdman and R. Kowarschik, "Testing of refractive silicon microlenses by use of a lateral shearing interferometer in transmission," *Appl. Opt.* **37**, 676-682 (1998).
11. F. Quercioli, B. Tiribilli, and M. Vassalli, "Wavefront-division lateral shearing autocorrelator for ultrafast laser microscopy," *Opt. Express* **12**, 4303-4312 (2004).
12. D. Mehta, S. Dubey, M. Hossain, and C. Shakher, "Simple multifrequency and phase-shifting fringe-projection system based on two-wavelength lateral shearing interferometry for three-dimensional profilometry," *Appl. Opt.* **44**, 7515-7521 (2005).
13. R. H. Hudgin, "Wave-front reconstruction for compensated imaging," *J. Opt. Soc. Am.* **67**, 375-378(1977).
14. D. L. Fried, "Least-squares fitting a wavefront distortion estimate to an array of phase-difference measurements," *J. Opt. Soc. Am.* **67**, 370-375(1977).
15. B. R. Hunt, "Matrix formulation of the reconstruction of phase values from phase differences," *J. Opt. Soc. Am.* **69**, 393-399(1979).
16. W. H. Southwell, "Wavefront estimation from wavefront slope measurements," *J. Opt. Soc. Am.* **70**, 998-1006 (1980).

17. K. R. Freischlad and C. L. Koliopoulos, "Modal estimation of wave front from difference measurements using the discrete Fourier transform," *J. Opt. Soc. Am. A* **3**, 1852-1861(1986).
 18. G. Harbers, P. J. Kunst and G. W. R. Leibbrandt, "Analysis of lateral shearing interferograms by use of Zernike polynomials," *Appl. Opt.* **35**, 6162-6172(1996).
 19. X. Tian and T. Yatagai, "Simple algorithm for large-grid phase reconstruction of lateral-shearing interferometry," *Appl. Opt.* **34**, 7213-7220(1995).
 20. H. von Brug, "Zernike polynomials as basis for wave-front fitting in lateral shearing interferometry," *Appl. Opt.* **36**, 2788-2790(1997).
 21. M. Servin, D. Malacara, and J. L. Marroquin, "Wave-front recovery from two orthogonal sheared interferograms," *Appl. Opt.*, **35**, 4343-4348(1996).
 22. C. Elster and I. Weingartner, "Exact wave-front reconstruction from two lateral shearing interferograms," *J. Opt. Soc. Am. A* **16**, 2281-2285(1999).
 23. C. Elster, and I. Weingartner, "Solution to the shearing problem," *Appl. Opt.* **38**, 5024-5031 (1999).
 24. C. Elster, "Exact two-dimensional wave-front reconstruction from lateral shearing interferograms with large shears," *Appl. Opt.*, **39**, 5353-5359(2000).
 25. A. Dubra, C. Paterson, and C. Dainty, "Wavefront reconstruction from shear phase maps using the discrete Fourier transform," *Appl. Opt.* **43**, 1108-1113 (2004).
 26. S. Okuda, T. Nomura, K. Kazuhide, H. Miyashiro, H. Hatsuzo, and K. Yoshikawa, "High precision analysis of lateral shearing interferogram using the integration method and polynomials," *Appl. Opt.*, **39**, 5179-5186(2000).
 27. P. Hariharan, B. F. Oreb, and T. Eiju, "Digital phase-shifting interferometry: a simple error-compensating phase calculation algorithm," *Appl. Opt.* **26**, 2504-2505(1987).
 28. M. H. Takeda, H. Ina, and S. Kobayashi, "Fourier transforms method of fringe-pattern analysis for computer-based topography and interferometry," *J. Opt. Soc. Am.* **72**, 156-160 (1982).
 29. T. J. Flynn, "Two-dimensional phase unwrapping with minimum weighted discontinuity," *J. Opt. Soc. Am. A* **14**, 2692-2701(1997).
 30. J. C. Wyant, "Double frequency grating lateral shear interferometer," *Appl. Opt.* **12**, 2057-2060 (1973).
 31. K. Patorski, "Grating shearing interferometer with variable shear and fringe orientation," *Appl. Opt.* **25**, 4192-4198 (1986).
 32. G. W. R. Leibbrandt, G. Harbers, and P. J. Kunst, "Wave-front analysis with high accuracy by use of a double-grating lateral shearing interferometer," *Appl. Opt.* **35**, 6151-6161(1996).
 33. H. Schreiber and J. Schwider, "Lateral shearing interferometer based on two Ronchi phase gratings in series," *Appl. Opt.* **36**, 5321-5324 (1997).
-

1. Introduction

Lateral shearing interferometry measures phase difference of object wave-front to reconstruct the wave-front distribution and is a useful tool in many applications, where optic quality needs to be quantitatively evaluated [1-12]. Main drawback of lateral shearing interferometry is that the phase of the wave-front under test is indirectly embedded in interferograms and thus an inverse problem has to be solved to extract the original phase from shearing interferograms. A variety of approaches have been proposed to retrieve two-dimensional (2-D) wave-front from two phase difference maps in two orthogonal directions [13-26]. Depending on reconstruction process, some of methods presume a small shear amount, e.g., the shear must equal one sampling interval in the interferograms[13-19], and the others allow large shear[20-26]. In practice, we found that the method proposed by Tian and Yatagai [19] is an efficient and easy-implemented scheme. Their method, based on least-square fitting(LSQ), gives a simple analytical solution to phase retrieval and performs fairly well in the sense of reconstruction precision and computing burden such as memory and time costs. However, due to limitation of one-pixel shear, this method is not applicable to the lateral shearing interferometers which are not able to produce such a small shear. Furthermore, as pointed by Okuda *et al.*[26], the sensitivity of the interferograms is low for a small shear, a situation existing in the test of smooth surfaces of optic mirror; therefore a proper shear amount, e.g., 10~20% of the diameter of the wave-front, is preferred. Our aim in this paper is to improve the procedure of Tian and Yatagai so that it allows a large shear. This improved algorithm uses the Fourier transform to extract one-dimensional(1-D) profile estimate. Taking into account that the

smaller dimension of the data range of the phase difference compared with that of the original phase, a data extension procedure is conducted before the estimate computation, providing that the number of samples N along shearing direction is divisible by the shear amount s . Influence of shear amount on reconstruction accuracy is tested by numeric experiments, and performance on noise robustness is also evaluated. The 2-D surface profile of a microlens array is reconstructed by optical experiment, which is performed in a double-grating shearing interferometer. Numerical and optical test have confirmed the stability and accuracy of the proposed algorithm.

2. Principle

In a lateral shearing interferometer, the object wave-front interferes with its sheared copy, forming a shearing interferogram. Using proper phase extraction techniques, such as, e.g., phase-shifting, Fourier fringe analysis, and phase-unwrapping [27-29], one gets from the interferogram the phase difference along the direction of shear. The phase difference is the subtraction between the original phase and its sheared copy, and represents the wave-front slope information. For testing wave-fronts with no rotational symmetry, one needs two wave-front slopes along two orthogonal directions [30].

Denoting the phase difference in the x direction in the discrete form by $D_x(m, n)$, and $D_y(m, n)$ in the y direction, they relate to the original phase $\varphi(m, n)$ by

$$D_x(m, n) = \varphi(m, n) - \varphi(m - s, n). \quad m, n=0,1,2,\dots,N-1. \quad (1.a)$$

$$D_y(m, n) = \varphi(m, n) - \varphi(m, n - s). \quad m, n=0,1,2,\dots,N-1. \quad (1.b)$$

where N denotes the number of the sampling points along x or y direction, and s is the shear amount. After performing 1-D Fourier transforms for both side of Eq. (1.a) in the x direction and (1.b) in the y direction, respectively, we get

$$FT_x\{\varphi(m, n)\} = \frac{FT_x\{D_x(m, n)\}}{1 - \exp(-\frac{i2\pi v_x s}{N})}. \quad (2.a)$$

$$FT_y\{\varphi(m, n)\} = \frac{FT_y\{D_y(m, n)\}}{1 - \exp(-\frac{i2\pi v_y s}{N})}. \quad (2.b)$$

where FT_α represents a 1-D Fourier transform in the α direction, and v_α is the corresponding spatial frequency and spans in $(0, N-1)$. If v_α reaches a multiple of N/s , the denominator of the Eq. (2), also called shearing transfer function[22], becomes zero, leading to undetermined results; i.e., the Fourier spectral components of wave-front at these points are lost. To resolve this problem, we can replace the frequency components at these leaking points by the average value of the two adjacent points, i.e., e.g., in x -dimensional, letting $FT_x(m, n)=[FT_x(m+1, n)+FT_x(m-1, n)]/2$. Even though such processing may result in possible reconstruction error, this minor error is tolerable providing that the shear s is not so large that the number of these leaking points remains to be small, as discussed in detail in Section 3.

It seems as if the inverse Fourier transform of Eq. (2) will reconstruct original wave-front, a constant phase bias may, however, lie in each row of data matrix computed from x -directional phase difference and in each column of data matrix of y -directional phase difference. We recognize the distribution of inverse Fourier transform of the right side in Eq. (2) as the 1-D profile estimate of original phase, described by

$$f_x(m,n) = FT_x^{-1} \left\{ \frac{FT_x \{D_x(m,n)\}}{1 - \exp(-\frac{i2\pi v_x s}{N})} \right\}. \quad (3.a)$$

$$f_y(m,n) = FT_y^{-1} \left\{ \frac{FT_y \{D_y(m,n)\}}{1 - \exp(-\frac{i2\pi v_y s}{N})} \right\}. \quad (3.b)$$

We should add appropriate phase values into each row of x -directional profile $f_x(m,n)$ and into each column of y -directional profile $f_y(m,n)$ to compensate for the deviation. As a result, the 1-D profile estimates must fit the original phase in the following way

$$f_x(m,n) + c_n = \varphi(m,n) + N_x(m,n). \quad (4.a)$$

$$f_y(m,n) + d_m = \varphi(m,n) + N_y(m,n). \quad (4.b)$$

where c_n is the phase offset in the n -th row of the x -directional estimate and d_m the offset in the m -th column of the x -directional estimate, respectively, and $N_x(m, n)$ is the deviation of x -directional phase estimate from the real phase and $N_y(m, n)$ the y -directional error. Then, the task of wave-front reconstruction reduces to find optimal phase offsets c_n and d_n for the 1-D phase estimates, $f_x(m, n)$ and $f_y(m, n)$. We adopt the squared sum of $N_x(m, n)$ and $N_y(m, n)$ as a residual error measure for wave-front reconstruction. Minimization of this residual error will produce the optimal phase. Following the LSQ procedure proposed by Tian and Yatagai [19], we get phase offsets, c_n and d_m , expressed by

$$c_n = -\frac{1}{N} \sum_{n=0}^{N-1} \left[f_x(N-1,n) - f_y(N-1,n) \right] - \frac{1}{N} \sum_{m=0}^{N-1} \left[f_x(m,n) - f_y(m,n) \right] + \frac{1}{N^2} \sum_{m=0}^{N-1} \sum_{n=0}^{N-1} \left[f_x(m,n) - f_y(m,n) \right]. \quad (5.a)$$

$n = 0, 1, 2, \dots, N-1.$

$$d_m = \frac{1}{N} \sum_{n=0}^{N-1} \left[f_x(m,n) - f_y(m,n) \right] - \frac{1}{N} \sum_{n=0}^{N-1} \left[f_x(N-1,n) - f_y(N-1,n) \right] \quad (5.b)$$

$m = 0, 1, 2, \dots, N-2.$

$$d_{N-1} = 0. \quad (5.c)$$

The optimally reconstructed phase is then obtained through the following relation,

$$\varphi(m,n) = \frac{[f_x(m,n) + c_n] + [f_y(m,n) + d_m]}{2}. \quad (6)$$

However, here exists one more information ambiguity except for above mentioned spectral leaking. The overlapped region between the wave-front and its sheared copy has a smaller dimension along the shearing direction than that of the original wave-front. Therefore, for a phase distribution within a region of interest(ROI), the resulting phase difference spans

in a smaller region. This dimension reduction hinders the LSQ fitting from being directly applied to the measured data. We adopt a data pre-processing strategy, as described below, to alleviate this difficulty.

In fact, if the original phase $\varphi(m, n)$ distributes in the (ROI): $m, n \in [0, N-1]$, the resulting phase difference $D_x(m, n)$ can only distribute in a smaller region: $m \in [s, N-1]$ and $n \in [0, N-1]$; i.e., the dimension of the phase difference matrix is $N \times (N-s)$ other than the expected $N \times N$. Therefore, $D_x(m, n)$ is lack of $N \times s$ data when we calculate the 1-D wave-front estimate according to Eq.(3), and so is $D_y(m, n)$. To solve this problem, we extend the original phase $\varphi(m, n)$ periodically in x direction and y direction, respectively, i.e., let $\varphi(m+kN, n+lN) = \varphi(m, n)$, where k and $l = 1, 2, \dots$. If the dimension of the original phase distribution N is a multiple of the shear s , the following relationship is obtained:

$$\sum_{p=0}^{(N/s)-1} D_x(m+ps, n) = 0. \quad m=0,1,2, \dots, s-1; n=0,1,2, \dots, N-1. \quad (7.a)$$

$$\sum_{q=0}^{(N/s)-1} D_y(m, n+qs) = 0. \quad n=0,1,2, \dots, s-1; m=0,1,2, \dots, N-1. \quad (7.b)$$

Thus, the missing data of the phase difference can be filled in with

$$D_x(m, n) = -\sum_{p=1}^{N/s-1} D_x(m+ps, n). \quad m=0,1,2, \dots, s-1; n=0,1,2, \dots, N-1. \quad (8.a)$$

$$D_y(m, n) = -\sum_{q=1}^{N/s-1} D_y(m, n+qs). \quad n=0,1,2, \dots, s-1; m=0,1,2, \dots, N-1. \quad (8.b)$$

The above relations have also been obtained in Refs. 22 and 25. In this way, the dimension of phase difference data is modified so as to match the dimension of the ROI under the constraint that the shear s or N must be chosen so that N/s is an integer.

From above discussions we know that the dimension of the phase difference distribution is inherently less than that of the original phase distribution. Some loss of information in wave-front reconstruction is thus inevitable even after the data processing as described above. This issue has been addressed by Servin *et al* [21], who called it an ill-posed inverse problem. Obviously, the precision of reconstruction will decrease when the shear amount increases. However, this reconstruction error is fairly small as long as the shear is not too big. This property is confirmed in the following numeric test and optical experiment.

3. Computer simulation

To evaluate the reliability of the proposed algorithm, we use the following phase function $\varphi(x, y)$ for reconstruction simulation:

$$\varphi(x, y) = 2\pi \times [0.1665 \times (x^2 + y^2 - 2)(x^2 + y^2 + 1) - 0.8325 \times (x^2 - y^2) - 0.6660 \times (x^2 + y^2)(x^2 - y^2)]. \quad (9)$$

This function is a combination of the Zernike polynomials and is sampled on a 256x256 grid. The Zernike function is selected since it is most often used in imaging system evaluation and thus represents typical phase distributions. The phase distribution is plotted in Fig.1(a). The shear s is chosen to be 16 in the simulation and the phase differences in two orthogonal directions are plotted in Figs.1(b) and (c), respectively. Figure 1(d) shows the reconstructed phase. The deviation of the reconstructed from the original phase is computed, using the root mean square (RMS) and peak-to-valley (PV) value of deviation as the error measure. In the numeric result, the unit of error is converted to wavelength λ , taking into account that the 2π

radian is equivalent to an optical length of λ . In this numeric test, the RMS is $3.00 \times 10^{-7} \lambda$ and the PV value is $3.27 \times 10^{-4} \lambda$.

To study the influence of the shear amount on the reconstruction accuracy, we use different s in simulations. The numeric results of the reconstruction are presented in Table 1. From Table 1 we know that, as s increases, both RMS and PV increase, because the amount of missing data of the phase difference increases accordingly. This test also shows that if the shear amount is not over 64 (i.e., 1/4 of the ROI dimension in this case), the RMS is less than $\lambda/1000$ and the PV is not up to the magnitude order of $\lambda/10$. Of course, the shear 64 is not the limit for the tested phase; the largest shear amount of the tested phase can be $N/2$ because the sampling dimension should be a multiple of the shear amount. Other phase functions, including continuous and discontinuous phase distributions, are also tested and give similar results. Therefore, the simulation results confirm that the proposed algorithm can yield satisfactory reconstruction precision even for a fairly large shear.

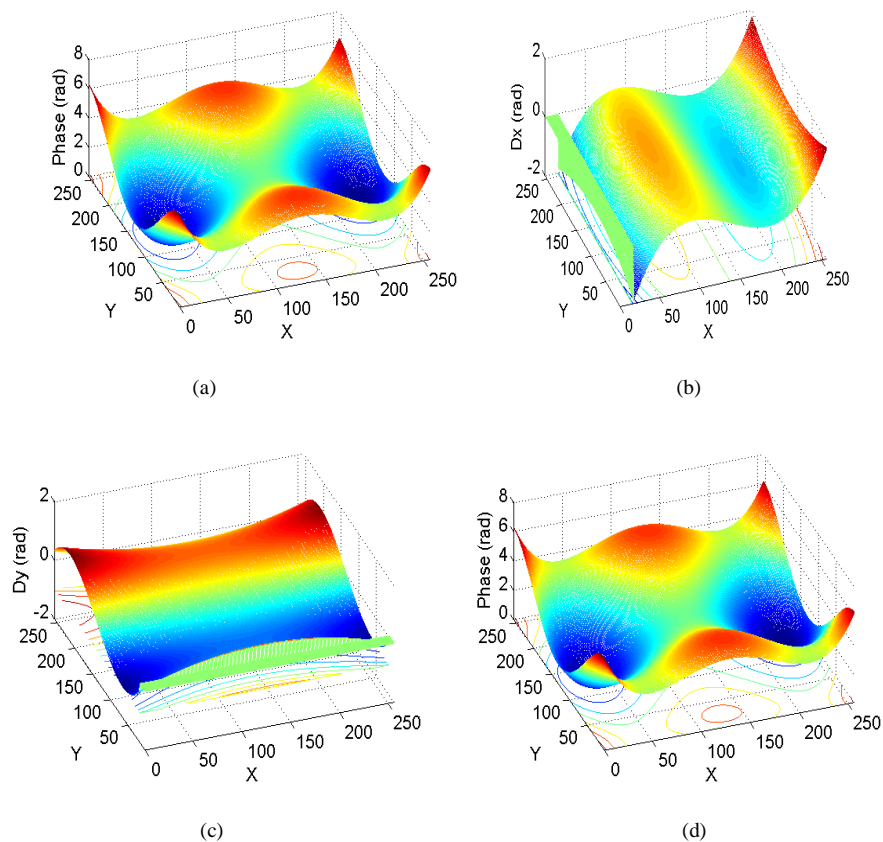


Fig. 1. Computer simulation of wave-front reconstruction from two phase differences in orthogonal directions: (a) is the original phase function, (b) and (c) are the x - and y -directional phase difference distributions, respectively, and (d) is the reconstructed phase distribution.

Table 1. Deviation of the reconstructed phase to the original phase vs. the shear amount s . ($\lambda=632.8\text{nm}$)

s (pixel)	2	4	8	16	32	64	128
RMS (λ)	4.67×10^{-9}	5.20×10^{-9}	6.33×10^{-8}	6.48×10^{-7}	1.25×10^{-5}	2.01×10^{-4}	5.20×10^{-3}
PV (λ)	-1.90×10^{-6}	-6.32×10^{-7}	2.65×10^{-5}	2.30×10^{-4}	2.00×10^{-3}	1.01×10^{-1}	3.32×10^{-1}

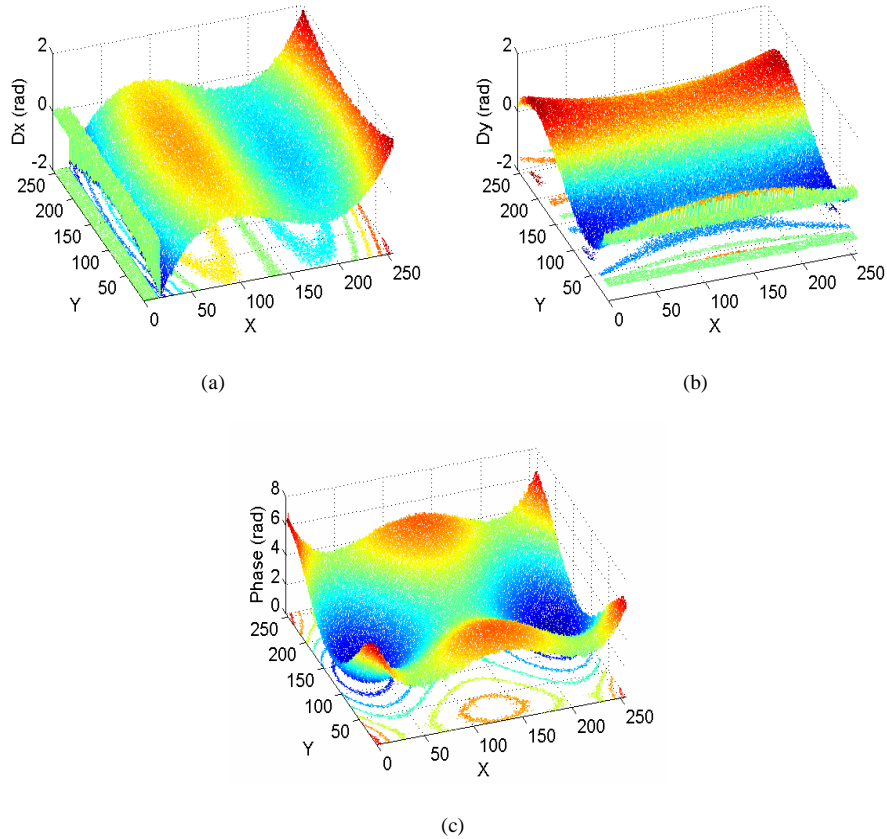


Fig. 2. Phase difference imposed by uniformly random noise with a level of 30%, where noise level is defined as the ratio between the average of noise absolute value and the one of the phase difference. (a) and (b) are the x- and y-directional phase difference distributions, respectively. (c) is the reconstructed phase distribution.

In lateral shearing interferometry, some noise may exist in the measured phase difference, due to, e.g., speckle, circumstance disturbance, detector noise, and other noise sources. To investigate the performance of the algorithm under noise circumstance, we add a uniformly distributed random noise into the phase differences. The noise level is denoted by the ratio between the average of noise absolute value and that of the phase difference. Figure 2 shows the wave-front reconstruction from the phase differences corrupted by a noise of level 30%. The reconstructed phase shown in Fig. 2(c) appears to be fairly good fidelity.

Figure 3 plots the RMS and the PV of the reconstructed phase vs. noise level. This example suggests that if the noise level is below 10%, the RMS is less than $\lambda/10^3$ and the PV is below $\lambda/10$, which is acceptable in interferometry practice.

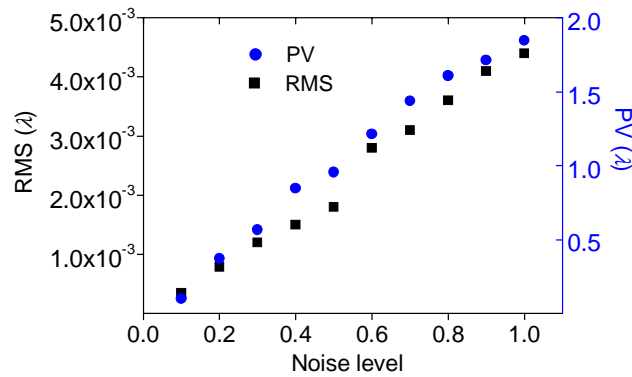


Fig. 3. Deviation of the reconstructed to the original phase vs. noise level, where noise level is defined as the ratio between the average of noise absolute value and the one of the phase difference

4. Optical experiment

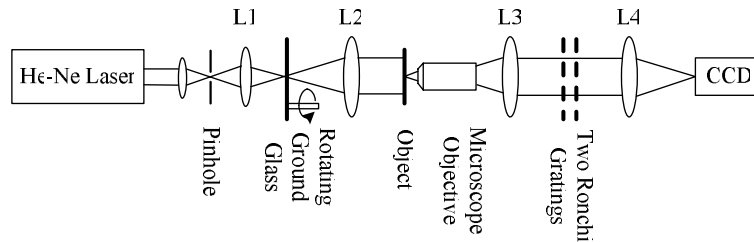


Fig. 4. Double-grating lateral shearing interferometer: Rotating ground glass is used to lower spatial coherence of the illumination light for reducing speckle; Two Ronchi gratings produce both shear and phase shift.

Shearing interference can be realized in many ways, among which the grating-based optical configuration is simple and easy-implemented[30-33], yielding shearing superposition of wave-fronts from the different diffraction orders of the grating. We carry out optical experiments in a double-grating lateral shearing interferometer, as shown in Fig. 4. The interferometer is common-path, and thus is immune from the vibration of the environment. The experimental configuration can also allow an illumination of low spatial coherence, which can greatly eliminate the bothersome speckle. As shown in the figure, a rotating ground glass is used for this purpose. In this system, the Rochi phase gratings can control both phase shift and shear. A PZT moves one of the gratings laterally for changing phase shift, and a desired shear is achieved by mechanically adjusting the distance between two gratings. The interferograms are captured by a CCD camera and sampled on a 512x512 grid. After acquiring a set of phase-shifted shearing interferograms in one direction, the gratings are rotated through 90 degree by a motor and the measurement in the perpendicular direction is carried out. Five interferograms with 5-step phase-shift are recorded, and then phase differences are extracted and unwrapped [27, 29].

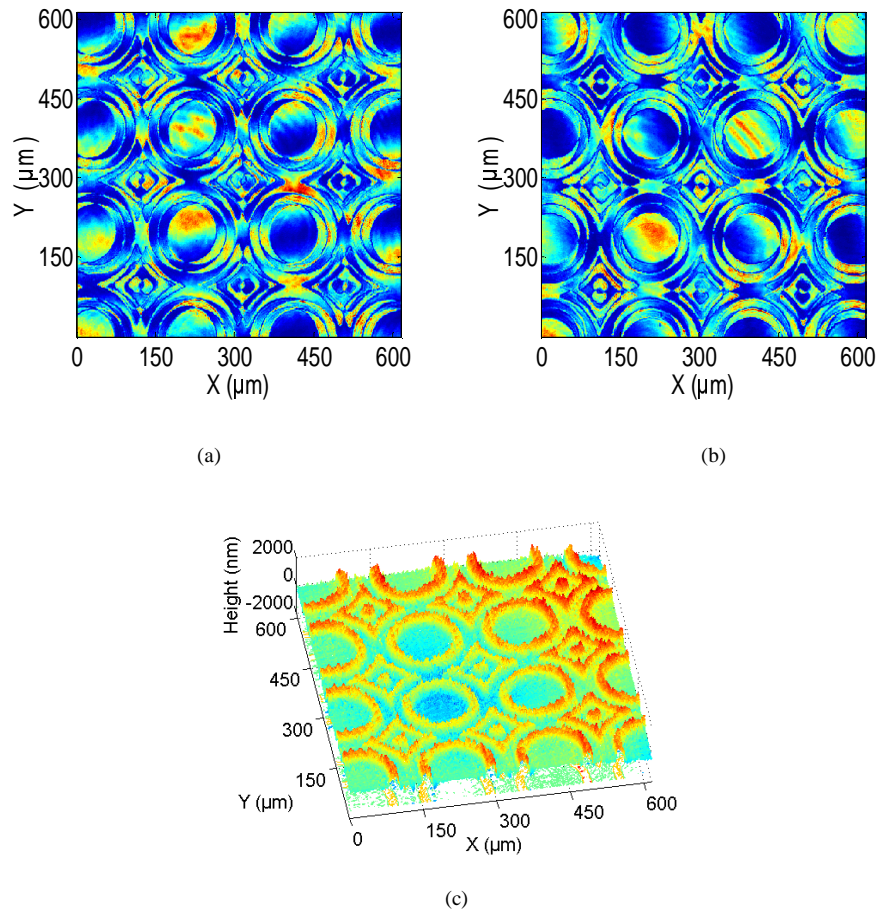


Fig. 5. Result of the optic surface testing with the double-grating lateral shearing interferometer. (a) The x-directional lateral-shearing interferogram. (b) The y-directional lateral-shearing interferogram. (c) The reconstructed phase distribution.

The object under test is a binary refractive microlens array which is produced by photo-etching quartz glass. The shearing interferograms resulting from the optical element are shown in Figs. 5(a) and 5(b). The shear amount is chosen to be 16. Some moiré stripes can be seen in Figs. 5(a) and 6(b). This is due to that the two Ronchi gratings are not perfectly parallel with each other. The orientation difference can be made as small as possible so that its influence on measurement accuracy could be neglected. The reconstructed 2-D phase is presented in Fig. 6(c). The depth d between the top and bottom of the binary relief of the element relates to the measured phase φ through $d = \lambda\varphi / (2\pi\Delta n)$, where the wavelength of the light source is $\lambda = 632.8$ nm and Δn is the difference between the refractive index of the glass and that of the air. The refractive index of the glass is 1.457 at the 632.8 nm wavelength. As a result, the relief height of the element is measured to be around 690 nm. For comparison, the step height is measured with the **Dektak 3** profilometer from **Veeco Instruments Inc.**. The measured value from the profiler is 630 nm, which yields a difference of about 10% between the two measurements. This may result from measuring process; the profilometer scans across only a line in a local area that is different from one tested by the interferometer.

5. Conclusion

We have developed an improved version of LSQ algorithm for reconstructing the 2-D wave-front reconstruction from shearing interferograms. This algorithm is applicable to cases in which the shear amount is larger than one sampling interval, and thus alleviates the limitation of the original algorithm. The algorithm can fulfill a fast phase reconstruction on the basis of that an analytic solution to LSQ is available and the 1-D profile estimate can be computed by the fast Fourier transform, and thus is simple and easy-implemented in terms of computation complexity and time-consuming. Using this method, we carried out optic surface testing in a double-grating lateral shearing interferometer and got the 3-D surface map of a binary optical element under test. The algorithm has shown good stability and reliability in wave-front reconstruction experiments, even under the situation of large shears and noisy interferograms. The only constraint of this method is that the sampling number along the shearing direction must be an integer multiple of the shear amount. This problem, however, can be resolved by using two lateral shearing interferograms with different shears [22]. The further study will be presented in a separate paper.

Acknowledgments

This work is supported in part by the NSFC under Grant Nos. 10474043 and 60290080. Corresponding author J.Ding's email address is jpding@nju.edu.cn.